Amino Acids
https://doi.org/10.1007/s00726-019-02704-7

ORIGINAL ARTICLE

Enzyme self-assembly on naked iron oxide nanoparticles for aminoaldehyde biosensing

Massimiliano Magro[1,2] · Davide Baratella[1] · Giovanni Miotto[3,4] · Jan Frömmel[5] · Marek Šebela[5] · Martina Kopečná[5] · Enzo Agostinelli[6,7] · Fabio Vianello[1,7]

Received: 9 August 2018 / Accepted: 16 January 2019

Abstract

The preservation of enzymatic activity is a fundamental requirement for exploiting hybrid nano-bio-conjugates, and the control over protein–nanoparticle interactions, leading to stable and catalytically active hybrids, represents the key for designing new biosensing platforms. In this scenario, surface active maghemite nanoparticles (SAMNs) represent a new class of naked magnetic nanoparticles, displaying peculiar electrocatalytic features and the ability to selectively bind proteins. Recombinant aminoaldehyde dehydrogenase from tomato (SlAMADH1) was used as a model protein, and successfully immobilized by self-assembly on the surface of naked SAMNs, where its enzymatic activity resulted preserved for more than 6 months. The hybrid nanomaterial (SAMN@SlAMADH1) was characterized by UV–Vis spectroscopy, mass spectrometry, and TEM microscopy, and applied for the development of a biosensor for the determination of aminoaldehydes in alcoholic beverages. Measurements were carried out in a low volume electrochemical flow cell comprising a SAMN modified carbon paste electrode for the coulometric determination of the NADH produced during the enzymatic catalysis. The present findings, besides representing the first example of an electrochemical biosensor for aminoaldehydes in an alcoholic matrix, open the door to the use of immobilized enzymes on naked metal oxides nanomaterials for biosensing.

Keywords Metal nanoparticles · Nanomaterial electrocatalysis · NADH electro-oxidation · Coulometric detection · Aminoaldehyde dehydrogenase · Aminoaldehyde biosensor

Abbreviations

APAL	3-Aminopropionaldehyde diethylacetal
CP	Carbon paste
CPE	Carbon paste electrode
CV	Cyclic voltammetry
FDR	False discovery rates
FTIR	Fourier-transform infrared
His-tag	Histidine-tag
IDA	Iminodiacetate
IPTG	Isopropyl β-D-1-thiogalactopyranoside
LB	Luria–Bertani
LC	Liquid chromatography
LOD	Limit of detection

Handling Editor: S. Beninati.

Electronic supplementary material The online version of this article (https://doi.org/10.1007/s00726-019-02704-7) contains supplementary material, which is available to authorized users.

✉ Fabio Vianello
fabio.vianello@unipd.it

[1] Department of Comparative Biomedicine and Food Science, University of Padua, Agripolis-Viale dell'Università 16, 35020 Legnaro, PD, Italy

[2] Regional Centre of Advanced Technologies and Materials, Department of Physical Chemistry, Faculty of Science, Palacký University in Olomouc, 17 Listopadu 12, 771 46 Olomouc, Czech Republic

[3] Department of Molecular Medicine, University of Padua, Via Gabelli 63, 35121 Padua, Italy

[4] Proteomic Center of Padua University, VIMM and Padua University Hospital, Via G. Orus 2b, 35129 Padua, Italy

[5] Department of Protein Biochemistry and Proteomics, Centre of the Region Haná for Biotechnological and Agricultural Research, Faculty of Science, Palacký University in Olomouc, Šlechtitelu 11, 78371 Olomouc, Czech Republic

[6] Department of Biochemical Sciences "A. Rossi Fanelli", University of Rome La Sapienza and CNR, Institute of Biology and Molecular Pathology, 00185 Rome, Italy

[7] International Polyamines Foundation-ONLUS, Via del Forte Tiburtino, 98, 00159 Rome, Italy

Published online: 06 February 2019

MGF	Mascot generic format
MS	Mass spectrometry
NADH	Nicotinamide adenine dinucleotide
Q-TOF	Quadrupole time of flight
RP	Reverse-phase
RSD	Relative standard deviation
SAMNs	Surface active maghemite nanoparticles
SlAMADH1	(*Solanum lycopersium*) aminoaldehyde dehydrogenase 1
SCE	Saturated calomel electrode
SD	Standard deviation
S/N	Signal/noise
TEM	Transmission electron microscopy
TRIS	Tris(hydroxymethyl)aminomethane
UV–Vis	Ultraviolet–visible
XRD	X-ray diffraction

Introduction

Innovative analytical techniques are currently proposed to control critical steps of an increasing variety of processes and in highly different environments (Rana et al. 2010). Nowadays, nano-bio-conjugates are important building blocks for developing novel analytical systems, with tailored characteristics, responding to specific requirements. Among all biomolecules, enzymes play a fundamental role in sensors development, and the possibility of firmly immobilizing enzymes, guaranteeing the retention of protein structure and function and minimizing the loss of their catalytic activity, is a main goal. A lot of efforts for the fine tuning nanoparticle–protein interfaces are ongoing (Mahmoudi et al. 2016), and an additional challenge is provided by systems, where the intimate contact between protein and nanoparticles is desirable, for example for optical and electronic systems.

A wide variety of core materials can be used for nanoparticles, including metals, metal oxides and semiconductors, which, in combination with biological macromolecules, are applicable for developing core–shell hybrids (He et al. 2015). The composition of the core material dictates the physical properties of the final nano-conjugate, and enzyme or protein coatings are responsible for catalytic and recognition peculiarities. Among reported examples, the binding of enzymes and proteins on nanoparticle surfaces was carried out by different chemistries, such as electrostatic interactions, physical adsorption and covalent immobilization by glutaraldehyde or carbodiimide linking reactions (Garcia et al. 2011; Niemirowicz et al. 2012). The immobilization of enzymes on nanostructured iron oxide is not so widespread, and generally only the crystalline form of magnetite was seriously taken into consideration (Netto et al. 2013). Nevertheless, several enzymes have been successfully immobilized onto iron oxide nanoparticles for electrochemical biosensing, e.g., lipases (Ren et al. 2011), horseradish peroxidase (Urbanova et al. 2014; Zhang et al. 2008), pectinase (Adalberto et al. 2012), trypsin (Kluchova et al. 2009), α-chymotrypsin (Xin et al. 2010), cyclic adenosine mono-phosphate-dependent protein kinase (Kwon et al. 2007), glucose oxidase (Baratella et al. 2013), S-formylglutathione hydrolase (Parracino et al. 2011), papain (Sahoo et al. 2013), alcohol dehydrogenase (Li et al. 2008; Urbanova et al. 2014), laccase (Rawal et al. 2012), amino oxidase (Bonaiuto et al. 2016) and epoxide hydrolase (Choi et al. 2010).

As prepared, uncoated magnetic nanoparticles suffer from their great proclivity to self-aggregate, which hampers the direct applications in aqueous solutions. Therefore, the surface of iron oxide nanoparticles must be modified to achieve desirable surface properties and functionalities. Thus, the interactions between the macromolecule and the nanoparticle will involve the nanomaterial coating, and the direct conjugation of nanoparticles to proteins remains an open problem.

Recently, we developed a new simple wet method to synthesize superparamagnetic nanoparticles constituted of stoichiometric maghemite (γ-Fe_2O_3) in the size range of around 10 nm, directly obtaining monodisperse preparations in aqueous media (Magro et al. 2012b). This new patented category of magnetic nanoparticles has been called "surface active maghemite nanoparticles" (SAMNs) because they are characterized by specific chemical behavior without any superficial modification or coating derivatization. Naked SAMNs are stable in water for several months as colloidal suspensions, present a high average magnetic moment and can be easily used to immobilize specific organic molecules in solution. Indeed, SAMN display a significantly positive zeta potential ($\zeta = +38.7 \pm 8.7$ mV) at pH 7.2, whereas reported nanostructured maghemite approaches the value of zero charge at the same neutral pH value, explaining the very low colloidal stability of the suspensions of common iron oxide nanomaterials (Lucas et al. 2007). To better appreciate this substantial difference, it should be considered that Patel and colleagues classified aqueous suspensions of nanoparticles as highly unstable, relatively stable, moderately stable and highly stable, with respect to the following zeta-potential (ζ) ranges: 0 to ± 10 mV, ± 10 to ± 20 mV and ± 20 to ± 30 mV and $^{>}\pm 30$ mV, respectively (Patel and Agrawal 2011). Thus, according to this scale, SAMNs suspensions can be considered as high stable, while all reported maghemite nanoparticles can be considered as unstable in water. Actually, the "Surface active" term indicates that SAMNs are able to form stable colloidal suspensions at neutral pH without any surfactant or surface stabilizer. This can be explained in terms of electrostatic repulsion between the nanoparticles in water. The availability and reactivity of under-coordinated iron(III) atoms on nanoparticle surface define the distinctive properties of SAMNs, and some

achievements were obtained leading to applications (Magro et al. 2015a, b). Moreover, a correlation between the tertiary structure of proteins and their affinity for SAMN surface was evidenced (Venerando et al. 2013; Magro et al. 2018), namely, strongly interacting proteins do not need to adapt their structure to bind on nanoparticle surface, thus their structure and their biological activity are not subjected to alterations.

In the present work, tomato (*Solanum lycopersicum*) aminoaldehyde dehydrogenase 1 (SlAMADH1), with a broad specificity towards ω-aminoaldehydes and aldehydes, was used. The binding of SlAMADH1 led to a stable hybrid material, (SAMN@SlAMADH1), and the enzymatic activity, colloidal stability and magnetic properties of the nano-bio-conjugate were exploited for the development of a coulometric biosensor, based on the complete enzymatic oxidation of aminoaldehyde substrates and leading to the concomitant formation of NADH inside a low volume electrochemical flow cell, with optimized reactant diffusion. After the catalysis, the enzymatic nanocarrier was captured by the application of an external magnet, making it available for reutilization. The low volume electrochemical flow cell comprised also a simple SAMN modified carbon paste electrode (SAMN/CPE) for the coulometric determination of the NADH produced during the enzymatic catalysis. The direct electro-oxidation of NADH coenzyme at the SAMN modified electrode completed a cost-effective detection system, which, considering the main focus of the study, shows good analytical performances.

The biosensor was tested on real samples without any sample preparation procedure and results suggest that SAMNs could be a promising, low cost, platform for the development of nano-bio-conjugates.

The novelty of the proposed approach is represented by the possibilities offered by the knowledge of the surface chemistry of nanomaterials for the engineering of nanoparticle–protein interfaces.

Materials and methods

Chemicals

Chemicals were purchased at the highest commercially available purity and were used without further treatment. Iron(III) chloride hexahydrate (97%), sodium borohydride ($NaBH_4$), ammonia solution (35% in water), nicotinamide adenine dinucleotides (NAD^+ and NADH) and 3-aminopropionaldehyde diethylacetal (APAL) were obtained from Aldrich (Sigma-Aldrich, Italy).

A series of Nd–Fe–B magnets (N35, 263–287 kJ/m^3 BH, 1170–1210 mT flux density by Powermagnet—Germany) was used for the magnetic driving of nanoparticles.

Preparation of aminoaldehyde dehydrogenase

The T7 express *Escherichia coli* strain carrying a pCDF-Duet vector with the SlAMADH1 gene (GenBank accession no. AY796114) was used for heterologous expression (Frömmel et al. 2012). Cells were grown at 30 °C in LB medium containing streptomycin to reach an optical density of about 0.6. Expression was then induced by isopropyl β-D-1-thiogalactopyranoside (IPTG, 0.1 mM) and the culture was incubated at 20 °C overnight. The produced protein carrying an N-terminal His-tag was then extracted and purified on Co-(II)-IDA-Sepharose according to a previous protocol developed for another recombinant plant enzyme of this group (Tylichová et al. 2010). The specific activity of the free enzyme was 4.35 U/mg protein.

Spectrophotometric assay for SlAMADH1

The enzymatic activity of SlAMADH1 was checked by a spectrophotometric assay, with APAL as a substrate. The NADH produced during APAL oxidation was monitored at 340 nm, under continuous stirring, and quantified using an extinction coefficient, ε, of 6220 $M^{-1}cm^{-1}$. The activity measurements were carried out in 100 mM TRIS/HCl, pH 8.5, containing 100 mM KCl, in the presence of 1.0 mM NAD^+. The enzymatic activity of the native and immobilized enzymes were determined by measuring their catalytic activity as a function of substrate concentration (APAL in the $10 - 1000 \times 10^{-6}$ M range), according to the Michaelis–Menten kinetic model (Fersht 1984). The catalytic constants were calculated by normalizing the measured substrate oxidation rate under saturation conditions (V_{max} at [S] ≫ Km) for the enzyme concentration. The concentration of SlAMADH1 immobilized on SAMNs was determined by mass spectrometry (see below).

Preparation of the SAMN@SlAMADH1 complex

The synthesis of iron oxide nanoparticles was already described (Magro et al. 2012b, c), and the nanoparticulated resulting material was characterized by ^{57}Fe zero field and in-field Mössbauer spectroscopy, FTIR spectroscopy, high resolution transmission electron microscopy, XRD, magnetization measurements (Magro et al. 2012a) and resulted in stoichiometric maghemite (γ-Fe_2O_3) with a mean diameter of 11 ± 2 nm, which can lead to the formation, upon ultrasound application in water (Bransonic, mod. 221, 48 kHz, 50 W) of a stable colloidal suspension, without any organic or inorganic coating or derivatization. Zeta potential (ζ) of neat SAMNs at room temperature in phosphate buffer (50 mM) at pH = 7.2 is + 38.7 ± 8.7 mV (Magro et al. 2017). The surface of these bare maghemite nanoparticles shows peculiar binding properties and can be reversibly derivatized

with selected organic molecules. We called these bare nanoparticles as Surface Active Maghemite Nanoparticles (SAMNs).

The immobilization of SlAMADH1 was obtained by self-assembly in water. For the immobilization of SlAMADH1 on SAMN surface, the binding reaction was performed by adding 13.6 μM SlAMADH1 to a SAMN suspension (0.5 mg mL^{-1}), under end-over-end mixing at 4.0 °C. As the enzyme binding process can be compromised by the presence of iron(III) chelating specie in solution, due to the competition for SAMN surface, phosphate ions and carboxylic acids were carefully eliminated using ultrapure water. Loosely bound enzyme was removed by repeated nanoparticle washing cycles, with the aid of an external magnet. The presence of the biomolecule in the supernatant was checked by the above mentioned spectrophotometric assay. After three washing cycles, the activity of the immobilized enzyme was constant and no detectable enzyme release was observed in the solution (residual activity in the washing buffer was less than 1%).

Mass spectrometry

SlAMADH1 samples, native or bound on SAMNs, were extensively dialyzed against 40 mM ammonium bicarbonate (3 × 2 h buffer changes with a 1000:1 volume ratio), dried under vacuum and re-suspended in 100 μL of 40 mM ammonium bicarbonate. Native and SAMN bound protein samples were incubated overnight at 37 °C with sequencing grade trypsin (Promega, Madison, WI, USA) and with a 120 (w/w) enzyme to substrate ratio. After tryptic digestion, samples were centrifuged at 14,000×*g* for 10 min and exposed to an external magnet for 30 min to remove SAMNs. Finally, the supernatant was dried under vacuum, dissolved in 20 μL of 0.1% formic acid and analyzed by LC–MS/MS using a 6520 Q-TOF mass spectrometer, coupled online with a 1200 series HPLC system through a Chip Cube Interface (Agilent Technologies, CA, USA). Each sample (4 μL) was loaded onto a C18 large capacity chip column, which integrates a 160 nL capacity trap column, an RP column (75 μm × 150 mm), connection capillaries, and a nano-spray emitter. Solvent A was water/0.1% formic acid, while solvent B was acetonitrile/0.1% formic acid. Peptides were separated with a linear gradient of 0–50% of solvent B in 50 min, at a flow rate of 0.3 μL min^{-1}. Mass spectra were acquired in a data dependent mode: MS/MS spectra of the 4 most intense ions were acquired for each MS scan in the range of 350–3000 Da. Scan speed was set to 2 MS spectra s^{-1} and 2 MS/MS spectra s^{-1}. Capillary voltage was set to 1850 V and drying gas to 5 L s^{-1}. Raw data files were converted into Mascot Generic Format (MGF) files with MassHunter Qualitative Analysis Software (Agilent Technologies). MGF files were analyzed using Mascot Search Engine server version 2.3 (Matrix Science, London, UK). Spectra were searched against the SwissProt database (May 2011 version, Taxonomy Mammalia, 65,453 entries) with the following parameters: enzyme specificity was set to trypsin up to 2 missed cleavages, peptide and fragment tolerance were set to 6 ppm and 0.05 Da respectively. Oxidation of methionine was selected as variable modification. False Discovery Rates (FDR) of 0.1%, based on the search against the corresponding randomized database, was calculated. The eight most relevant peptides (see Table 1 and Fig. 1B of the main text) originated from trypsin digestion of native and immobilized SlAMADH1, identified with a confidence ≥ 99%, were used to quantify the amount of enzyme bound to nanoparticles surface.

Table 1 Quantification of the amount of SlMADH1 bound to SAMNs

	Peptide	MASCOT score	Peak signal from 50 fmol of free SlMADH1	Peak signal from SlMADH1 bound on 150 ng SAMN
1	NVPIPR	37	1,012,451	1,584,389
2	SVLATLESLDSGK	80	533,444	999,012
3	ISFTGSGPTGSK	66	732,254	1,394,892
4	TEEQAIELANDTK	91	152,793	258,076
5	MTPVNLNSDSYK	71	662,132	1,265,536
6	YGLGAAVMSK	74	816,527	1,367,394
7	TFKTEEQAIELANDTK	93	314,729	659,163
8	QVTEYTSAEPLAFYK	99	219,586	375,359
	Peak signal sum		4,443,916	7,903,821 (yields 592.8 fmol, which is 32.5 μg SlAMADH1 per mg of SAMN)

The amount of bound SlMADH1 was calculated by comparison of total intensity of the eight most relevant peptides obtained after trypsin digestion of native (50 fmol) and SAMN (150 ng)-bound SlMADH1

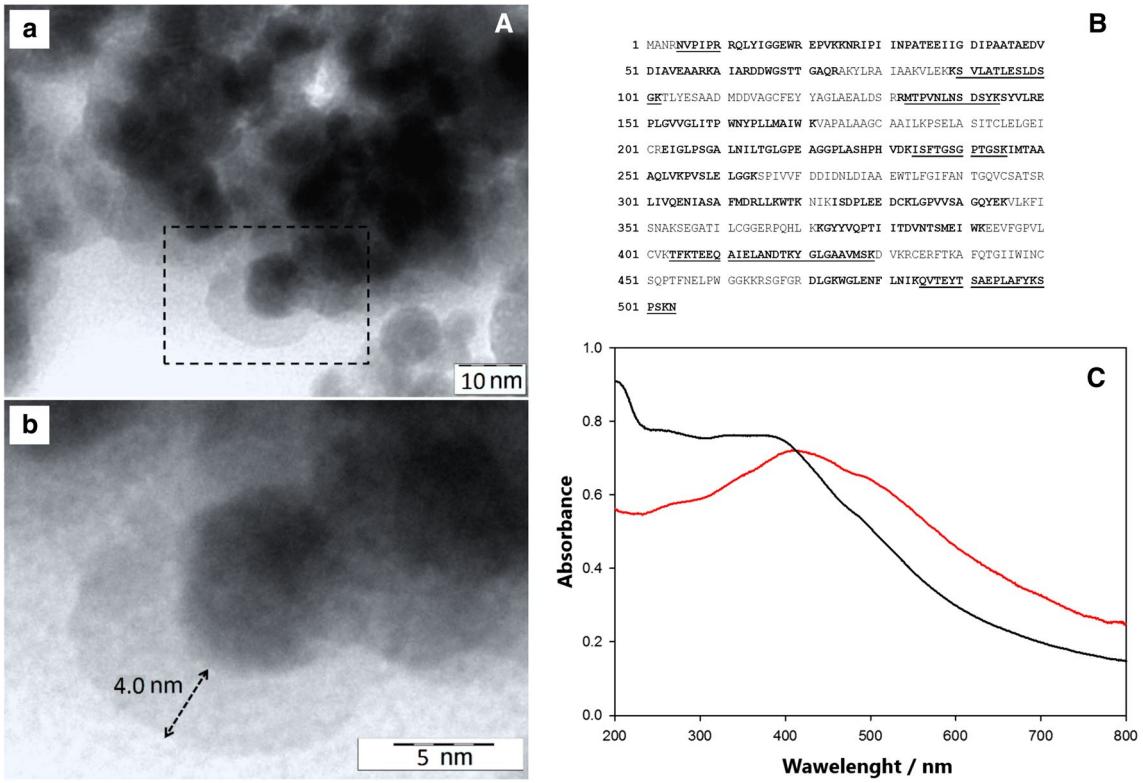

Fig. 1 Structural characterization of the SAMN@SlAMADH1 nano-bio-conjugate and amino acid sequence of SlAMADH1. **A** TEM micrograph of the SAMN@SlAMADH1 nano-bio-conjugate, (a) TEM micrograph of the SAMN@SlAMADH1 nano-bio-conjugate. (b) An enlarged portion of (a), where the thickness of the organic shell (SlAMADH1) around the inorganic nanoparticle core (SAMN) has been highlighted by an arrow; **B** mass spectrometry coverage of SlAMADH1, where underlined regions were used for quantification; **C** absorption spectra of SAMNs and SAMN@SlAMADH1 suspensions. The spectra were acquired in a 1 cm quartz cuvette in water (black line) SAMN; (red line) SAMN@SlAMADH1

Results

Characterization of SAMN@SlAMADH1 complex

The immobilization of SlAMADH1 was carried out by self-assembly in water (see "Materials and methods" section), an optimized process exploiting the affinity of a specific protein for SAMN surface (Magro et al. 2012a; Venerando et al. 2013). Protein affinity for the nanomaterial depends on the availability of sterically compatible chelating groups on protein surface (Magro et al. 2018), and is strictly correlated with the preservation of the enzyme tertiary structure and biological activity.

The amount of SlAMADH1 immobilized on SAMNs was determined by mass spectrometric analysis. The mass profile of the tryptic digestion of native and bound enzymes yielded a sequence coverage of 61% (Fig. 1B). The eight most representative peptides, characterized by a Mascot score > 35 ($p < 0.01$) and accounting for about 15% of the sequence coverage, were quantitatively compared to calculate the amount and specific activity of bound SlAMADH1 (Table 1), which resulted 0.35 U/mg protein. Mass spectrometry results indicated 32.47 ± 5.52 µg SlAMADH1 mg^{-1} SAMNs corresponding to about 4 enzyme molecules per nanoparticle. For comparison, the possible theoretical number of SlAMADH1 molecules on SAMN surface was calculated, considering the protein adhering on a sphere of about 5 nm radius by its widest side. With this approximation, 7 SlAMADH1 molecules per nanoparticle, in a close packed geometry, were obtained. This result approximated SlAMADH1 surface, at the interface with SAMNs, as an ellipse of about 45 nm^2 area completely covering the 314 nm^2 nanoparticle surface. However, no protein–protein hindrance was considered. Moreover, the adhesion of the whole side surface of SlAMADH1 on SAMNs should induce a distortion of protein tertiary structure, as it should adapt to the nanoparticle curvature. Such a protein deformation upon binding would be in contrast with the retention of enzymatic activity. In addition, the possible repulsion between different proteins should be considered. Therefore, 4 SlAMADH1 molecules per SAMN is a reasonable value for maximum enzyme absorption per nanoparticle, considering an absorption process not involving alterations of protein tertiary structure.

TEM micrographs showed an organic shell around electron-dense SAMNs (Fig. 1A). The fraction of organic phase coating the nanoparticle surface is clearly reflected in the observed shell thickness (approx. 4 nm) and in the lower contrast of the nanoparticles themselves, which are more embedded into the protein matrix. The shell thickness appeared very close to SlAMADH1 size. While SAMN@SlAMADH1 in water maintains its colloidal behavior for a long time, the witnessed aggregated character of the coated nanoparticles in the TEM screening (Fig. 1A) results from the pre-treatment and drying of the aqueous sample on the holey-carbon/copper-mesh grid prior the measurements.

The SAMN@SlAMADH1 complex was further studied by optical spectroscopy. The absorption spectrum of naked SAMNs, acquired in water, shows a wide band with a maximum at about 400 nm (Fig. 1C) characterized by an extinction coefficient of 1520 $M^{-1}cm^{-1}$ (expressed as Fe_2O_3 molar concentration, considering the iron oxide molar mass of 160 g mol^{-1}). The interaction of SlAMADH1 with SAMN surface induced an alteration of the nanoparticle optical properties (see Fig. 1C). Upon SlAMADH1 binding, both the shape and position of maximum absorption were altered with respect to bare SAMNs, confirming the influence of SAMN surface properties on optical characteristics as already described (Magro et al. 2012a, 2014, 2015a). In water, the spectrum of SAMN@SlAMADH1 was characterized by a peak at 410 and a shoulder at 498 nm (see Fig. 1C). According to the surface reconstruction theory (Rajh et al. 2002), such a red shift can be attributed to the modification of nanoparticle surface due to a covalent ligand.

It is worth reminding that, due to the robustness of the stoichiometric maghemite nanocrystals, the inherent properties of the maghemite core (i.e. superparamagnetism) were always preserved as extensively demonstrated by different techniques, such as magnetization measurements, Mossbauer spectroscopy and high resolution electron transmission microscopy, and upon the reaction with different surface modifiers (Magro et al. 2012b, 2015a, b).

Finally, a comparison of the enzymatic activity of native SlAMADH1 and SAMN@SlAMADH1, under the same experimental conditions, indicates that SlAMADH1 was successfully immobilized on SAMNs, showing a detectable catalytic activity on APAL. In particular, the specific activity of the immobilized enzyme was 0.35 U/mg protein. In comparison with the native enzyme, K_m values were 41.1 and 180 µM for native SlAMADH1 and SAMN@SlAMADH1, respectively. Whereas, under our experimental conditions (18.5 µg mL^{-1} native SlAMADH1 and 2.0 mg mL^{-1} SAMN@SlAMADH1, corresponding to about 65.0 µg mL^{-1} SlAMADH1), V_{max} values were 80.36 and 12.14 µM min^{-1}, respectively.

Moreover, SAMN@SlAMADH1 maintained its catalytic activity over repeated magnetic separation and resuspension cycles, demonstrating the reusability of this magnetic drivable nano-catalyst. The catalytic activity of SAMN@SlAMADH1 resulted preserved upon 6 months storage at 4.0 °C, and the enzymatic activity measured before and after this period were superimposable.

Electrochemical characterization

According to previous experiences (Baratella et al. 2013; Magro et al. 2013), a carbon paste electrode was modified with naked SAMNs (SAMN/CPE) (see Materials and Methods in Supplementary Material), and characterized by cyclic voltammetry in the −0.8 to +0.8 V vs. SCE applied potential range.

Measurements were carried out in a conventional electrochemical cell (3 mL) in the absence or in the presence of NADH, showing an increase of both capacitive and the faradic current with NADH and evidencing the peculiar electrocatalytic properties of SAMNs toward the direct electrooxidation of NADH. For comparison, measurements were also acquired with an un-modified carbon paste electrode (see Fig. 2a). In particular, CVs of CPEs in the absence of SAMNs resulted superimposable before and after the addition of NADH, indicating that no redox process occurred. Whereas, CVs of SAMN doped CPEs showed a concentration dependent increase of the faradic current upon the addition of the electroactive substance. SAMN electrocatalysis was not accompanied by the appearance of a redox wave, plausibly because of the high irreversibility and the mechanism complexity of the redox reaction.

The carbon paste electrode modified with SAMNs permitted the chronoamperometric determination, at relatively low applied potential, of NADH produced during the oxidation of aminoaldehydes by SAMN@SlAMADH1.

The chronoamperometric response, acquired at +0.4 V vs. SCE, as a function of NADH additions, is reported in Fig. 2b. From the calibration with NADH, the detection limit was determined (0.85 µM, S/N = 3), and the typical response time, between 10 and 95% of steady-state response, was calculated (70 s). The electrode sensitivity was estimated (21.52 nA $\mu M^{-1}cm^{-2}$, $R > 0.996$) (see the calibration curve reported in the inset of Fig. 2b).

A low volume flow electrochemical cell was developed to detect at completion the electroactive substances produced by the enzymatic activity of the SAMN@SlAMADH1 hybrid nano-conjugate (see Materials and Methods in Supplementary Material). Thus, this new cell configuration was electrochemically characterized. The cell setup is reported in Fig. 3a and electrochemical measurements were carried out in the confined small solution volume (1 µL geometrical volume), using SAMN/CP as working electrode and conventional electrodes: counter (platinum) and reference (Ag/AgCl). The thinness of the solution

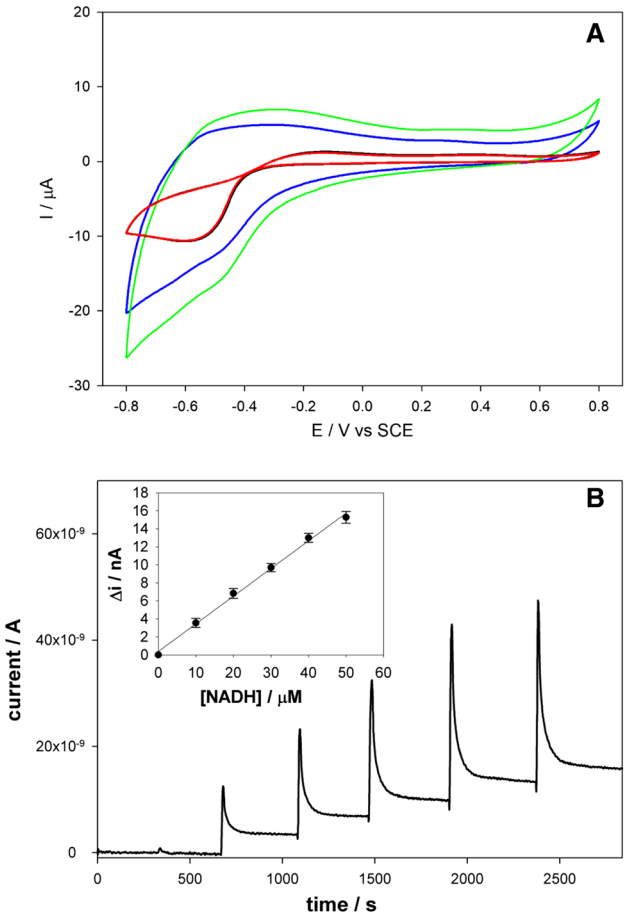

Fig. 2 Electrochemical characterization of carbon paste electrodes modified with SAMNs toward the electro-oxidation of NADH. **a** Cyclic voltammogramms of CPE and SAMN/CPE. Measurements were carried out in a conventional electrochemical cell in 100 mM TRIS–HCl, pH 8.5, containing 100 mM KCl as supporting electrolyte, equilibrated with air, in the presence or absence of 0.5 mM NADH: (black line) CPE; (red line) CPE, 0.5 mM NADH; (blue line) SAMN/CPE; (green line) SAMN/CPE, 0.5 mM NADH; **b** Chronoamperometry carbon paste electrode modified with SAMNs following the addition of NADH. Measurements were carried out in 100 mM TRIS–HCl, pH 8.5, containing 100 mM KCl as supporting electrolyte, equilibrated with air, at 0.4 V (vs. SCE). Inset: calibration curve of the SAMN/CPE with NADH

layer inside the low volume electrochemical cell permitted the fast diffusion of electroactive compounds toward the electrode surface.

The coulometric behavior of the cell was evaluated by injecting solutions containing various concentrations of NADH in the range from 25 µM to 2.0 mM. After NADH injection, the potential was applied and swept from 0 to + 1.2 V, vs. Ag/AgCl, at 2 mV/s, and a current peak was obtained (see Fig. 3b). Under these conditions, the oxidation peak was observed at about + 700 mV. By integrating the peak area, the corresponding total amount of NADH present in the microcell was calculated, supposing that 2 electrons were transferred during the oxidation of NADH according to the following reaction: $NADH + H^+ \rightarrow NAD^+ + 2e^- + 2H^+$.

The calibration curve was linear ($r \geq 0.99$) up to 2 mM NADH (see the inset of Fig. 3b), being 0.105 ± 0.0017 µC μM^{-1} NADH the sensitivity. For each NADH concentration, the standard deviation of repetitive measurements ($n \geq 5$) was below 4.8%. A calibration plot was also built injecting NADH into the electrochemical cell containing the SAMN@SlAMADH1, and no significant differences were observed.

On the basis of NADH calibration plot, the cell volume was confirmed according to the following equation (Eq. 1):

$$q = zFcV, \quad (1)$$

where q is the total reduction charge, $z = 2$ is the number of electrons transferred during the oxidation of NADH, F the Faraday constant, c the NADH concentration and V is the cell volume. The cell volume was 0.544 µL.

Application of SAMN@SlAMADH1 for the development of a biosensor for aminoaldehydes

Hereafter, we present a biosensor for aminoaldehyde/aldehyde detection, in which SAMN@SlAMADH1 (20 mg mL^{-1}) was applied as catalytic element and carbon paste electrode modified with naked SAMNs (SAMN/CPE) was employed as an electrochemical transducer for the enzymatically produced NADH. A schematic representation of the working principle and the operational phases of SAMN@SlAMADH1 based biosensor are presented in Fig. 4a, b. In Fig. 5, an example of the coulometric determination of APAL is reported. A calibration plot as a function of APAL concentration was built, showing a sensitivity of 5.33 µC μM^{-1} cm^{-2} and a limit of detection (LOD) of 750 nM (see Fig. 5, inset) was calculated according to the following eqn (Eq. 2):

$$LOD = (3 \times SD)/m, \quad (2)$$

where SD is the standard deviation of 5 electrode responses in the absence of the analyte and m is the slope of the calibration curve. The linearity range was 25 µM–2.0 mM APAL. The whole measurement time, taking into account the completion of the enzymatic reaction (15–20 min) and the potential sweep, was estimated in 25–30 min.

Additionally, the repeatability of biosensor response was calculated on 5 repetitive analyses of 400 µM APAL and standard deviation resulted below 4%. Moreover, biosensor reproducibility was evaluated by testing the system performances following $n = 4$ electrode surface renewals, consisting in the complete removal of the electrode material (1.0 mm thickness) from the electrochemical cell and its substitution with fresh material. The reproducibility RSD

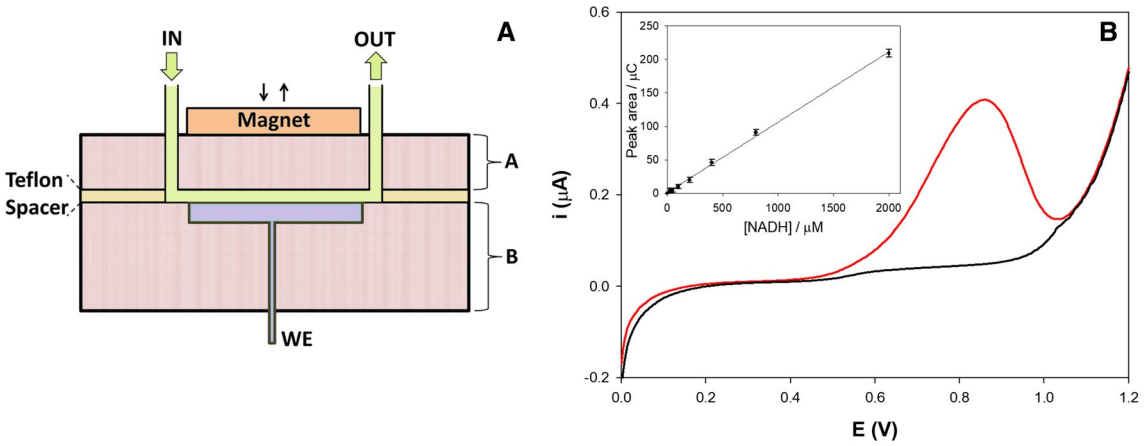

Fig. 3 Schematic drawing of the electrochemical flow cell and calibration with NADH. **a** The cell (not in scale) is equipped with a carbon paste electrode modified with 15% SAMN. Between the two half cells (**a** and **b**) a channel was defined by a Teflon spacer. A moveable magnet is placed on the top; **b** linear sweep voltammetry acquired with the electrochemical flow microcell (black line) following the addition of NADH (red line). Measurements were carried out in 100 mM TRIS–HCl, pH 8.5, containing 100 mM KCl as supporting electrolyte, equilibrated with air. Inset: calibration curve with NADH

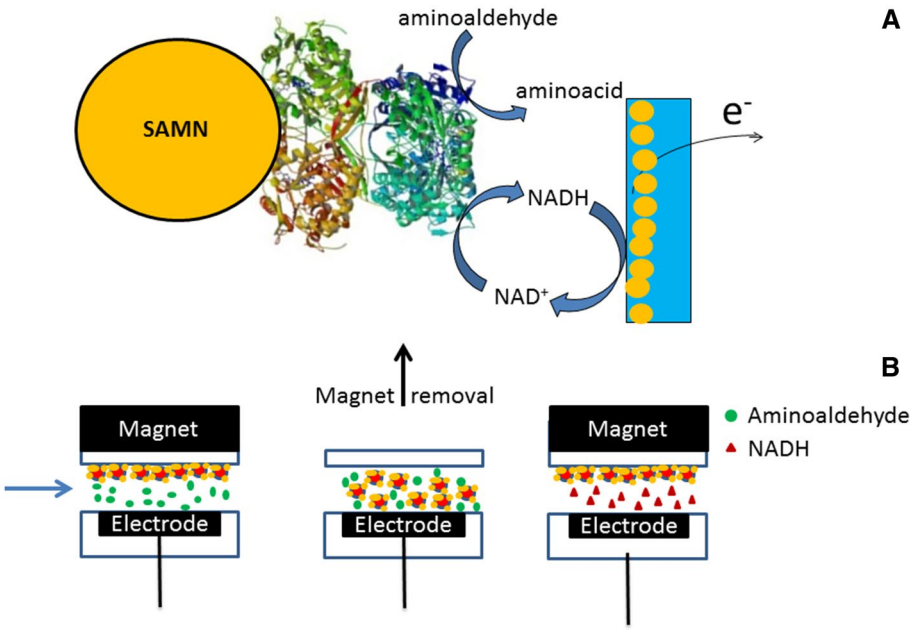

Fig. 4 Biosensor for aminoaldehydes/aldehydes: **a** simplified scheme of the biosensor working principle; **b** provides a schematic representation of the operational phases of the biosensor based on the magnetically drivable biological element (SAMN@SlAMADH1)

value was comparable with the value reported for repeatability (5.0%).

Finally, the biosensor was tested on real samples of distilled beverages (slivovitz, i.e. a plum brandy) that may contain aminoaldehydes and aldehydes as a part of the fusel oil. Slivovitz samples, were injected in the electrochemical flow cell, in which SAMN@SlAMADH1 complexes were previously blocked by a Nd–Fe–B magnet. After sample injection, the magnet was removed, permitting the completion of the enzymatic reaction. Then, a potential sweep was applied at the working electrode and produced NADH was volumetrically determined. The total fusel oil aminoaldehyde concentration determined by the biosensor in slivovitz samples was 1.403 ± 0.1 mM (calculated using APAL as reference) being close to the value obtained by the spectrophotometric activity assay (1.27 ± 0.15 mM) (Frömmel et al. 2016). The measurements were performed on three samples in triplicate.

Discussion

SAMNs are able to recognize and bind selected proteins in complex biological systems (Venerando et al. 2013; Magro et al. 2018). Moreover, strongly interacting proteins do

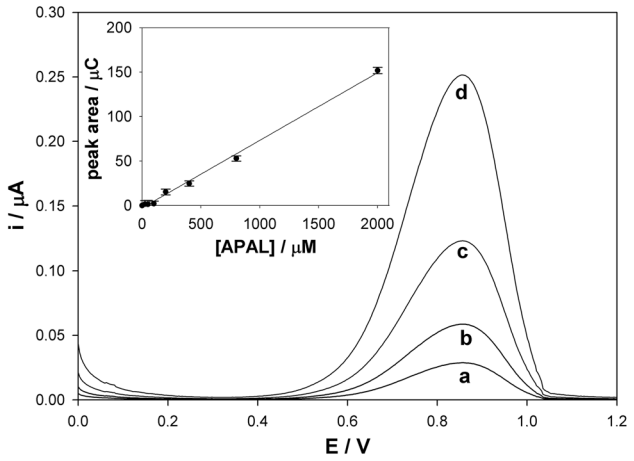

Fig. 5 Linear sweep voltammetry acquired with the electrochemical flow microcell (reported in Fig. 3a) following the addition of APAL. Measurements were carried out in 100 mM TRIS–HCl, pH 8.5, containing 100 mM KCl as supporting electrolyte, equilibrated with air. a 200.0 μM; b 400.0 μM c 800.0 μM; d 2000.0 μM. The inset shows calibration plot made as a function of APAL concentration

not need to adapt their structure upon the interaction, thus their biological activity is preserved in the final conjugate (Venerando et al. 2013; Magro et al. 2018). The affinity of proteins for this peculiar nanomaterial has been recently explained in term of distribution of carboxylic groups matching the topography of under-coordinated iron(III) on SAMN surface (Magro et al. 2018). Indeed, in the SAMN size domain, the surface atoms adjust their coordination environment to form under-coordinated metal sites, and ligand binding is favored because of ligand adsorption induces a restructuration of the nanoparticle surface. Rajh and colleagues initially applied this paradigm, named surface reconstruction theory, to explain the change of the optical characteristics of metal oxide nanoparticles due to the binding of enediol ligands (Rajh et al. 2002). This approach can be effectively used for nanomaterials displaying good colloidal stability, high crystallinity, and dimensions below 20 nm. In our previous studies were introduced some progresses on surface reconstruction theory, demonstrating that the effect of protein binding on the optical spectrum of nanoparticles provides evidences on the protein corona formation by surface reconstruction mechanism (Magro et al. 2012a; Venerando et al. 2013; Magro et al. 2015a). Herein, the self-assembly of the hybrid nanomaterial (SAMN@SlAMADH1) was successfully highlighted by UV–Vis spectroscopy and characterized by mass spectrometry and TEM microscopy.

The preservation of the enzymatic activity of SAMN@SlAMADH1 further substantiate that SlAMADH1 was successfully immobilized on SAMNs, showing a detectable catalytic activity on APAL. In comparison to the native enzyme, SlAMADH1 conjugated to SAMNs showed a lower activity. This is not an unusual outcome for immobilized enzymes (Chong and Zhao 2004; Pan et al. 2009), indeed a reduction of the enzyme mobility can be plausibly expected upon covalent binding. Even if the role of conformational changes on enzyme catalytic properties is still controversial, it is believed that the alteration of the local environment and macromolecule flexibility can influence enzyme catalysis (Johnson 2008). Thus, the loss of protein flexibility, due to the covalent nature of the immobilization, can explain the observed decrease of the catalytic properties. On the other hand, it is well known that covalent immobilization can increase the stability of immobilized enzymes, minimizing protein leaching from the support (Misson et al. 2015). This is of particular importance as enzymatic activity and stability of nano-bioconjugates represent the main requirements for the reliability of any biotechnological application. In the present case, the covalent nature of the binding conferred a significant robustness to SAMN@SlAMADH1 as witnessed by the preserved catalytic activity over repeated magnetic separation and resuspension cycles and upon 6 months storage at 4.0 °C. Thus, the SAMN@SlAMADH1 conjugate showed suitable features for the development of a biosensor for aminoaldehydes and aldehydes. In the proposed system, SAMN@SlAMADH1 oxidized aminoaldehyde molecules with the concomitant production of NADH, and after the completion of the enzymatic reaction in the above described low volume cell, the nano-conjugate was finally captured by the application of the external magnet, making it available for reutilization. The as produced NADH was electro-oxidized on the surface of a carbon paste electrode modified with SAMNs. To note that the electrochemical oxidation of NADH represents an important drawback to overcome, mainly due to the slow electron transfer between NADH and electrodes, even at a potential, where the reaction is thermodynamically favorable (Radoi and Compagnone 2009). Moreover, it generally proceeds with coupled side reactions, poisoning the electrode surface (Samec and Elving 1983).

The proposed biosensor, being diffusion controlled the reaction between of SAMN@SlAMADH1 and the analyte within the cell volume, allows the total conversion of aminoaldehydes, and, working under coulometric regime, can be utilized without any calibration procedure. The successful application on distilled beverages (slivovitz, i.e. a plum brandy) witnesses the reliability of the nano-conjugate.

Finally, aminoaldehydes are toxic substances generated by the enzymatic oxidation of polyamines (see reaction Scheme 1). As polyamines are present in all biological matrixes, the potential risk of food contamination by aminoaldehydes is widespread.

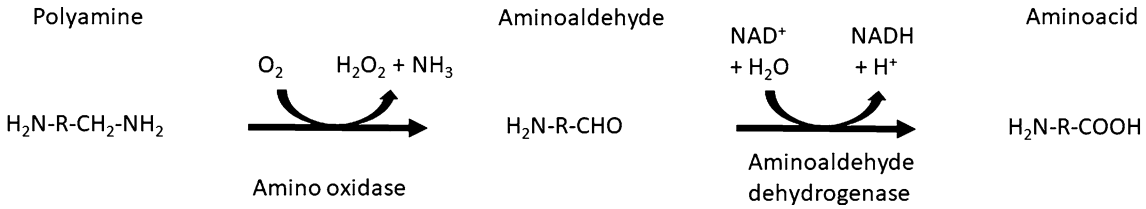

Scheme 1 Reaction scheme of the production and elimination of aminoaldehydes

Conclusions and perspectives

Polyamines are ubiquitous cell components, as well as aminoaldehydes, their oxidation products, and can be potentially present in many different biological matrixes depending on the availability of amino oxidases (see Scheme 1). Due to the toxicity of these last compounds, the development of versatile sensing platforms represent an important task nowadays. In particular, up to the author knowledge, an electrochemical sensor for the determination of amino aldehydes in alcoholic beverages has not already been reported.

Hybrid nanomaterials composed of inorganic nanoparticles and biological macromolecules are generally produced by conventional chemistries involving different hydrophilic coatings on nanomaterials surface to ensure water dispersion. Up to the author knowledge, no reports on the direct binding between an enzyme and naked iron oxide nanoparticles has been reported, where nanoparticle surface represents a friendly environment, guaranteeing the preservation of enzymatic activity. Therefore, this approach represents a novel strategy for designing catalytically active nano-conjugates for biotechnological applications. An enzyme, namely an aminoaldehyde dehydrogenase, was firmly immobilized on the surface of naked maghemite nanoparticles, preserving the catalytic activity, and leading to the formation of a SAMN@SlAMADH1 conjugate. The developed conjugate was applied for creating a novel biosensor, combining electrochemical features and binding properties of SAMNs.

The system shows a series of peculiarities: (a) a carbon paste electrode modified with naked SAMNs was used for the direct electro-oxidation of NADH; (b) The complete enzymatic oxidation of sample aldehydes or ω-aminoaldehydes by the SAMN@SlAMADH1 hybrid, producing the corresponding amount of NADH, was carried out in a colloidal suspension inside a low volume electrochemical flow cell optimizing reactant diffusion; (c) NADH, produced during the complete enzymatic oxidation of ω-aminoaldehydes or aldehydes, was coulometrically determined at the SAMN modified electrode; (d) the capture of the nano-conjugate (SAMN@SlAMADH1) by the application of an external magnet makes it available for reutilization.

The present work highlights the possibility to design and develop new nano-conjugates with tailored characteristics and responding to specific requirements by exploiting the specificity of the surface of peculiar iron oxide nanoparticles and envisaging the possibilities offered by SAMNs as an elective tool for the developing of innovative biosensing systems.

Acknowledgements The present experimental work was partially funded by Italian Institutional Ministry Grants Cod. 60A06-7411 and 60A06-8055. The authors gratefully acknowledge the University of Padua (Italy), Grant PRAT 2015 (progetti di Ateneo) n. CPDA159850 and the CARIPARO Foundation for the support. The team members from the Czech Republic were supported by Grant No. LO1204 from the Ministry of Education, Youth and Sports. The authors also thank 'La Sapienza' University of Rome and Italian MIUR (Ministero dell'Istruzione, dell'Università e della Ricerca). Our gratitude is also due to the "International Polyamine Foundation-ONLUS" for the availability to look up in the Polyamines documentation.

Compliance with ethical standards

Conflict of interest The authors declare that they have no conflicts of interest with the contents of this article.

Research involving human participants and/or animals This article does not contain any studies with human participants or animals performed by any of the authors.

References

Adalberto PR, José dos Santos F, Golfeto CC, Costa Iemma MR, Ferreira de Souza DH, Cass QB (2012) Immobilization of pectinase from *Leucoagaricus gongylophorus* on magnetic particles. Analyst 137:4855–4859. https://doi.org/10.1039/C2AN35682A

Baratella D, Magro M, Sinigaglia G, Zboril R, Salviulo G, Vianello F (2013) A glucose biosensor based on surface active maghemite nanoparticles. Biosens Bioelectron 45:13–18. https://doi.org/10.1016/j.bios.2013.01.043

Bonaiuto E, Magro M, Baratella D, Jakubec P, Sconcerle E, Terzo M, Miotto G, Macone A, Agostinelli E, Fasolato S, Venerando R, Salviulo G, Malina O, Zboril R, Vianello F (2016) Ternary hybrid γ-Fe_2O_3/Cr^{VI}/amine oxidase nanostructure for electrochemical sensing: application for polyamine detection in tumor tissue. Chem Eur J 22:1–8. https://doi.org/10.1002/chem.201600156

Choi SH, Kim HS, Lee IS, Lee EY (2010) Functional expression and magnetic nanoparticle-based immobilization of a protein-engineered marine fish epoxide hydrolase of *Mugil cephalus* for enantioselective hydrolysis of racemic styrene oxide. Biotechnol Lett 32:1685–1691. https://doi.org/10.1007/s10529-010-0335-4

Chong ASM, Zhao XS (2004) Design of large-pore mesoporous materials for immobilization of penicillin G acylase biocatalyst. Catal Today 93–95:293–299. https://doi.org/10.1016/j.cattod.2004.06.064

Fersht A (1984) Enzyme structure and mechanism. W.H. Freeman & Co, New York

Frömmel J, Soural M, Tylichová M, Kopečný D, Demo G, Wimmerová M, Šebela M (2012) Plant aminoaldehyde dehydrogenases oxidize a wide range of nitrogenous heterocyclic aldehydes. Amino Acids 43:1189–1202. https://doi.org/10.1007/s00726-011-1174-x

Frömmel J, Tarkowski P, Kopečný D, Šebela M (2016) The use of tomato aminoaldehyde dehydrogenase 1 for the detection of aldehydes in fruit distillates. New Biotechnol 33:666–675. https://doi.org/10.1016/j.nbt.2015.11.010

Garcia J, Zhang Y, Taylor H, Cespedes O, Webb ME, Zhou D (2011) Multilayer enzyme-coupled magnetic nanoparticles as efficient, reusable biocatalysts and biosensors. Nanoscale 3:3721–3730. https://doi.org/10.1039/C1NR10411J

He C, Liu D, Lin W (2015) Nanomedicine applications of hybrid nanomaterials built from metal–ligand coordination bonds: nanoscale metal–organic frameworks and nanoscale coordination polymers. Chem Rev 115:11079–11108. https://doi.org/10.1021/acs.chemrev.5b00125

Johnson KA (2008) Role of induced fit in enzyme specificity: a molecular forward/reverse switch. J Biol Chem 283:26297–26301. https://doi.org/10.1074/jbc.R800034200

Kluchova K, Zboril R, Tucek J, Pecova M, Zajoncova L, Safarik I, Mashlan M, Markova I, Jancik D, Sebela M, Bartonkova H, Bellesi V, Novak P, Petridis D (2009) Superparamagnetic maghemite nanoparticles from solid-state synthesis-their functionalization towards peroral MRI contrast agent and magnetic carrier for trypsin immobilization. Biomaterials 30:2855–2863. https://doi.org/10.1016/j.biomaterials.2009.02.023

Kwon HS, Han KC, Hwang KS, Lee JH, Kim TS, Yoon DS, Yang EG (2007) Development of a peptide inhibitor-based cantilever sensor assay for cyclic adenosine monophosphate-dependent protein kinase. Anal Chim Acta 585:344–349. https://doi.org/10.1016/j.aca.2006.12.037

Li GY, Huang KL, Jiang YR, Yang DL, Ding P (2008) Preparation and characterization of Saccharomyces cerevisiae alcohol dehydrogenase immobilized on magnetic nanoparticles. Int J Biol Macromol 42:405–412. https://doi.org/10.1016/j.ijbiomac.2008.01.005

Lucas IT, Durand-Vidal S, Dubois E, Chevalet J, Turq P (2007) Surface charge density of maghemite nanoparticles: role of electrostatics in the proton exchange. J Phys Chem C. 111:18568–18576

Magro M, Faralli A, Baratella D, Bertipaglia I, Giannetti S, Salviulo G, Zboril R, Vianello F (2012a) Avidin functionalized maghemite nanoparticles and their application for recombinant human biotinyl-SERCA purification. Langmuir 28:15392–15401. https://doi.org/10.1021/la303148u

Magro M, Sinigaglia G, Nodari L, Tucek J, Polakova K, Zdeněk M, Cardillo S, Salviulo G, Russo U, Zboril R, Stevanato R, Vianello F (2012b) Charge binding of rhodamine derivative to OH– stabilized nanomaghemite: universal nanocarrier for construction of magnetofluorescent biosensors. Acta Biomater 8:2068–2076. https://doi.org/10.1016/j.actbio.2012.02.005

Magro M, Baratella D, Pianca N, Toninello A, Grancara S, Zboril R, Vianello F (2013) Electrochemical determination of hydrogen peroxide by isolated mitochondria: a novel nanocomposite carbon-maghemite nanoparticle electrode. Sens Actuators B Chem 176:315–322. https://doi.org/10.1016/j.snb.2012.09.044

Magro M, Campos R, Baratella D, Lima G, Hola K, Divoky C, Stollberger R, Malina O, Aparicio C, Zoppellaro G, Zboril R, Vianello F (2014) A magnetically drivable nanovehicle for curcumin with antioxidant capacity and MRI relaxation properties. Chem Eur J 20:11913–11920. https://doi.org/10.1002/chem.201402820

Magro M, Baratella D, Jakubec P, Zoppellaro G, Tucek J, Aparicio C, Venerando R, Sartori G, Francescato F, Mion F, Gabellini N, Zboril R, Vianello F (2015a) Triggering mechanism for DNA electrical conductivity: reversible electron transfer between DNA and iron oxide nanoparticles. Adv Funct Mater 25:1822–1831. https://doi.org/10.1002/adfm.201404372

Magro M, Baratella D, Salviulo G, Polakova K, Zoppellaro G, Tucek J, Kaslik J, Zboril R, Vianello F (2015b) Core–shell hybrid nanomaterial based on prussian blue and surface active maghemite nanoparticles as stable electrocatalyst. Biosens Bioelectron 52:159–165. https://doi.org/10.1016/j.bios.2013.08.052

Magro M, Valle G, Russo U, Nodari L, Vianello F (2015c) Maghemite nanoparticles and method for preparing thereof. US Patent 8,980,218

Magro M, Martinello T, Bonaiuto E, Gomiero C, Baratella D, Zoppellaro G, Cozza G, Patruno M, Zboril R, Vianello F (2017) Covalently bound DNA on naked iron oxide nanoparticles: intelligent colloidal nano-vector for cell transfection. Biochim Biophys Acta 1861:2802–2810. https://doi.org/10.1016/j.bbagen.2017.07.025

Magro M, Zaccarin M, Miotto G, Da Dalt L, Baratella D, Fariselli P, Gabai G, Vianello F (2018) Analysis of hard protein corona composition on selective iron oxide nanoparticles by MALDI-TOF mass spectrometry: identification and amplification of a hidden mastitis biomarker in milk proteome. Anal Bioanal Chem 410:2949–2959. https://doi.org/10.1007/s00216-018-0976-z

Mahmoudi M, Bertrand N, Zope H, Farokzad OC (2016) Emerging understanding of the protein corona at the nano-bio interfaces. Nano Today 11:817–832. https://doi.org/10.1016/j.nantod.2016.10.005

Misson M, Zhang H, Jin B (2015) Nanobiocatalyst advancements and bioprocessing applications. J R Soc Interface 12:20140891. https://doi.org/10.1098/rsif.2014.0891

Netto CGCM, Toma HE, Andrade LH (2013) Superparamagnetic nanoparticles as versatile carriers and supporting materials for enzymes. J Mol Catal B 85–86:71–92. https://doi.org/10.1016/j.molcatb.2012.08.010

Niemirowicz K, Markiewicz KH, Wilczewska AZ, Car H (2012) Magnetic nanoparticles as new diagnostic tools in medicine. Adv Med Sci 57:196–207. https://doi.org/10.2478/v10039-012-0031-9

Pan C, Hu B, Li W, Sun Y, Ye H, Zeng X (2009) Novel and efficient method for immobilization and stabilization of β-D-galactosidase by covalent attachment onto magnetic Fe_3O_4–chitosan nanoparticles. J Mol Catal B Enz 61:208–215. https://doi.org/10.1016/j.molcatb.2009.07.003

Parracino A, Gajula GP, di Gennaro AK, Neves-Petersen MT, Rafaelse J, Petersen SB (2011) Towards nanoscale biomedical devices in medicine: biofunctional and spectroscopic characterization of superparamagnetic nanoparticles. J Fluoresc 21:663–672. https://doi.org/10.1007/s10895-010-0754-6

Patel VR, Agrawal YK (2011) Nanosuspension: an approach to enhance solubility of drugs. J Adv Pharm Technol Res 2:81–87. https://doi.org/10.4103/2231-4040.82950

Radoi A, Compagnone D (2009) Recent advances in NADH electrochemical sensing design. Bioelectrochemistry 76:126–134. https://doi.org/10.1016/j.bioelechem.2009.06.008

Rajh T, Chen LX, Lukas K, Liu T, Thurnauer MC, Tiede DM (2002) Surface restructuring of nanoparticles: an efficient route for ligand–metal oxide crosstalk. J Phys Chem B 106:10543–10552. https://doi.org/10.1021/jp021235v

Rana S, Yeh YC, Rotello VM (2010) Engineering the nanoparticle-protein interface: applications and possibilities. Curr Opin Chem Biol 14:828–834. https://doi.org/10.1016/j.cbpa.2010.10.001

Rawal R, Chawla S, Pundir DCS (2012) An amperometric biosensor based on laccase immobilized onto Fe_3O_4NPs/cMWCNT/PANI/Au electrode for determination of phenolic content in tea

leaves extract. Enzyme Microb Technol 51:179–185. https://doi.org/10.1016/j.enzmictec.2012.06.001

Ren Y, Rivera JG, He L, Kulkarni H, Lee DK, Messersmith PB (2011) Facile, high efficiency immobilization of lipase enzyme on magnetic iron oxide nanoparticles via a biomimetic coating. BMC Biotechnol 11:63–70. https://doi.org/10.1186/1472-6750-11-63

Sahoo B, Sahu SK, Bhattacharya D, Dhara D, Pramanik P (2013) A novel approach for efficient immobilization and stabilization of papain on magnetic gold nanocomposites. Coll Surf B Biointerfaces 101:280–289. https://doi.org/10.1016/j.colsurfb.2012.07.003

Samec Z, Elving PJ (1983) Anodic oxidation of dihydronicotinamide adenine dinucleotide at solid electrodes; mediation by surface species. J Electroanal Chem 144:217–234. https://doi.org/10.1016/S0022-0728(83)80157-0

Tylichová M, Kopečný D, Moréra S, Briozzo P, Lenobel R, Snégaroff J, Šebela M (2010) Structural and functional characterization of plant aminoaldehyde dehydrogenase from *Pisum sativum* with a broad specificity for natural and synthetic aminoaldehydes. J Mol Biol 396:870–882. https://doi.org/10.1016/j.jmb.2009.12.015

Urbanova V, Magro M, Gedanken A, Baratella D, Vianello F, Zboril R (2014) Nanocrystalline iron oxides, composites, and related materials as a platform for electrochemical, magnetic, and chemical biosensors. Chem Mater 26:6653–6673. https://doi.org/10.1021/cm500364x

Venerando R, Miotto G, Magro M, Dallan M, Baratella D, Bonaiuto E, Zboril R, Vianello F (2013) Magnetic nanoparticles with covalently bound self-assembled protein corona for advanced biomedical applications. J Phys Chem C 117:20320–20331. https://doi.org/10.1021/jp4068137

Xin BJ, Si SF, Xing GW (2010) Protease immobilization on γ-Fe_2O_3/Fe_3O_4 magnetic nanoparticles for the synthesis of oligopeptides in organic solvents. Chem Asian J 5:1389–1394. https://doi.org/10.1002/asia.200900696

Zhang HL, Lai GS, Han DY, Yu AM (2008) An amperometric hydrogen peroxide biosensor based on immobilization of horseradish peroxidase on an electrode modified with magnetic dextran microspheres. Anal Bioanal Chem 390:971–977. https://doi.org/10.1007/s00216-007-1748-3